The Cellulose Synthase Gene Superfamily and Biochemical Functions of Xylem-Specific Cellulose Synthase-Like Genes in *Populus trichocarpa*[1][W][OA]

Shiro Suzuki[2], Laigeng Li, Ying-Hsuan Sun, and Vincent L. Chiang*

Forest Biotechnology Group, Department of Forestry and Environmental Resources, College of Natural Resources, North Carolina State University, Raleigh, North Carolina 27695

Wood from forest trees modified for more cellulose or hemicelluloses could be a major feedstock for fuel ethanol. Xylan and glucomannan are the two major hemicelluloses in wood of angiosperms. However, little is known about the genes and gene products involved in the synthesis of these wood polysaccharides. Using *Populus trichocarpa* as a model angiosperm tree, we report here a systematic analysis in various tissues of the absolute transcript copy numbers of cellulose synthase superfamily genes, the cellulose synthase (*CesA*) and the hemicellulose-related cellulose synthase-like (*Csl*) genes. Candidate *Csl* genes were characterized for biochemical functions in Drosophila Schneider 2 (S2) cells. Of the 48 identified members, 37 were found expressed in various tissues. Seven *CesA* genes are xylem specific, suggesting gene networks for the synthesis of wood cellulose. Four *Csl* genes are xylem specific, three of which belong to the *CslA* subfamily. The more xylem-specific *CslA* subfamily is represented by three types of members: *PtCslA1*, *PtCslA3*, and *PtCslA5*. They share high sequence homology, but their recombinant proteins produced by the S2 cells exhibited distinct substrate specificity. PtCslA5 had no catalytic activity with the substrates for xylan or glucomannan. *PtCslA1* and *PtCslA3* encoded mannan synthases, but *PtCslA1* further encoded a glucomannan synthase for the synthesis of (1→4)-β-D-glucomannan. The expression of *PtCslA1* is most highly xylem specific, suggesting a key role for it in the synthesis of wood glucomannan. The results may help guide further studies to learn about the regulation of cellulose and hemicellulose synthesis in wood.

Most of the biomass produced in trees is the secondary xylem, or wood. Cellulose and hemicelluloses represent almost the entire polysaccharide components in walls of the secondary xylem cells (Sarkanen and Hergert, 1971; Higuchi, 1997). Lignin is the third major wall component of these cells. Wood in angiosperm trees generally contains 42% to 50% cellulose, 25% to 30% hemicelluloses, 20% to 25% lignin, and 5% to 8% extractives (Fengel and Wegener, 1984). Xylan and glucomannan comprise approximately 85% and 15% of the total hemicellulose, respectively (Timell, 1969; Fengel and Wegener, 1979, 1984). This lignocellulosic pool is a major carbon sink in forest ecosystems and accounts for roughly 20% of the terrestrial carbon storage (Schlesinger and Lichter, 2001), offering an enormous, renewable polysaccharide feedstock for materials and biofuels (Ragauskas et al., 2006). Trees are target energy crops in the United States (Wooley et al., 1999; McAloon et al., 2000).

Being abundant in wood, cellulose, xylan, and glucomannan can be readily purified for structure characterization. Cellulose is a linear polymer composed of (1→4)-linked β-D-Glc residues. Xylan is a polymer with a linear backbone composed entirely of β-D-Xyl residues connected through (1→4)-linkages and is partially acetylated and substituted with 4-*O*-methyl-GlcUA groups (Perila, 1961; Timell, 1964, 1969; Fengel and Wegener, 1984; Jacobs et al., 2002). Xylan in angiosperm wood is therefore also referred to as *O*-acetyl-4-*O*-methylglucuronoxylan. Glucomannan in angiosperm wood is essentially a pure linear polymer containing (1→4)-linked β-D-Glc and β-D-Man residues, with Glc:Man ratios of 1:1 to 1:3 (Timell, 1986; Jacobs et al., 2002).

Profiling of gene transcript abundances during cotton (*Gossypium hirsutum*) fiber development resulted in the identification of the first plant cellulose synthase (*CesA*) gene (Pear et al., 1996). Arabidopsis (*Arabidopsis thaliana*) cellulose-deficient mutants allowed further cloning of a number of *CesA* genes and characterizing the genetic functions of *CesA* genes. *CesA* genes encode membrane proteins (Brown and Montezinos, 1976;

[1] This work was supported by the Japan Society for the Promotion of Science (2004–2006; postdoctoral fellowship for research abroad to S.S.), by the National Research Initiative of the U.S. Department of Agriculture Cooperative State Research, Education, and Extension Service (grant no. 2004–35504–14652 to V.L.C.), and by the North Carolina State University Forest Biotechnology Industrial Research Consortium (grant no. 524450 to L.L. and S.S.).

[2] Present address: Institute of Sustainability Science, Kyoto University, Gokasho, Uji, Kyoto 611–0011, Japan.

* Corresponding author; e-mail vincent_chiang@ncsu.edu; fax 919–515–7801.

The author responsible for distribution of materials integral to the findings presented in this article in accordance with the policy described in the Instructions for Authors (www.plantphysiol.org) is: Vincent L. Chiang (vincent_chiang@ncsu.edu).

[W] The online version of this article contains Web-only data.

[OA] Open Access articles can be viewed online without a subscription.

www.plantphysiol.org/cgi/doi/10.1104/pp.106.086678

Kimura et al., 1999; Dhugga, 2001; Doblin et al., 2002). Among the 10 *CesA* genes identified in the Arabidopsis genome (Richmond and Somerville, 2000), *AtCesA8*, *AtCesA7*, and *AtCesA4*, corresponding to *irx1*, *irx3*, and *irx5* mutants, are believed to coordinate cellulose biosynthesis in the secondary walls (Taylor et al., 1999, 2000, 2003; Gardiner et al., 2003). Biochemical functions of *CesA* genes have not been determined, nor has plant cellulose synthase activity been demonstrated (Doblin et al., 2002; Peng et al., 2002).

Hemicelluloses are believed to be synthesized in the Golgi, mediated most likely by cellulose synthase-like (Csl) proteins (Carpita and McCann, 2000). However, functions of Csl proteins are largely uncharacterized. CesA and Csl proteins belong to a cellulose synthase superfamily within the glycosyltransferase (GT) family 2 (Dhugga, 2001; Keegstra and Raikhel, 2001; Coutinho et al., 2003; Somerville et al., 2004). In Arabidopsis, there are at least six *Csl* gene subfamilies (A–G), containing 29 members (Richmond and Somerville, 2000; Hazen et al., 2002). The biosynthesis of cell wall hemicelluloses may involve some of these Csls for backbone elongation and other GTs for side-chain addition (Cutler and Somerville, 1997; Richmond and Somerville, 2000; Perrin et al., 2001; Hazen et al., 2002; Coutinho et al., 2003; Dhugga et al., 2004; Girke et al., 2004; Liepman et al., 2005). Only three such *GT* genes have demonstrated biochemical functions, all associated with the biosynthesis of Arabidopsis xyloglucan in the primary cell walls (Edwards et al., 1999; Perrin et al., 1999; Faik et al., 2002; Vanzin et al., 2002; Madson et al., 2003). Dhugga et al. (2004) first showed in guar (*Cyamopsis tetragonoloba*) seeds a gene encoding a β-mannan synthase (ManS) activity capable of synthesizing the $(1\rightarrow4)$-β-D-mannan backbone of galactomannan. The expression of this *ManS* (*CtManS*) gene is closely associated with guar endosperm development where the accumulation of galactomannan takes place (Dhugga et al., 2004). *CtManS* gene is in the *CslA* subfamily. Liepman et al. (2005) were the first to confirm the biochemical functions of Arabidopsis *CslA* genes (*AtCslA2*, *AtCslA7*, and *AtCslA9*) in Drosophila Schneider 2 (S2) cells and postulated that all plant *CslA* genes encode enzymes with ManS activity and that *AtCslA9* may also encode a β-glucomannan synthase (GlcManS). The tissue-specific expression of these *AtCslA* genes, however, was not reported. A recent genetic study showed evidence for the participation of rice (*Oryza sativa*), or more monocot-specific, *CslF* genes in the biosynthesis of cell wall $(1\rightarrow3;1\rightarrow4)$-$\beta$-D-glucans that are normally absent from dicot species (Burton et al., 2006).

Eighteen *CesA* genes were identified in the *Populus trichocarpa* genome (Djerbi et al., 2005), but *Csl* genes in this genome are poorly annotated. Only a handful of *CesA* and *Csl* genes from tree species were studied for their expression patterns (Wu et al., 2000; Samuga and Joshi, 2002; Liang and Joshi, 2004; Nairn and Haselkorn, 2005; Geisler-Lee et al., 2006; Ranik and Myburg, 2006). None of the tree *Csl* genes have been characterized for the biochemical functions to determine those involved in the synthesis of wood hemicelluloses. This is due mainly to the unavailability of efficient heterologous expression systems prior to the one developed by Liepman et al. (2005) and a lack of knowledge for identifying xylem- or wood-specific *Csl* genes for functional analysis. We carried out a systematic, genome-wide analysis of all the possible cellulose synthase superfamily members in *P. trichocarpa* for the phylogenetic relationship and for the quantitative transcript abundance in various tissues. These analyses led to the identification of xylem-specific *CslA* gene members, whose recombinant proteins were produced in Drosophila S2 cells. One member having the most conspicuous xylem specificity encoded a GlcManS for the synthesis of $(1\rightarrow4)$-β-D-glucomannan.

RESULTS

Cellulose Synthase Gene Superfamily in the *P. trichocarpa* Genome

We identified in the *P. trichocarpa* genome database (http://www.jgi.doe.gov/poplar/) 48 gene models encoding transmembrane and D,D,D,QxxRW (Saxena et al., 1995; Campbell et al., 1997; Saxena and Brown, 1997) domains containing full protein sequences that are homologous to the Arabidopsis CesA and Csl proteins. Sequence analysis using the BLASTX program (Altschul et al., 1997) suggested that, of these 48 genes, 18 could be classified as *CesA* genes and were denoted as *PtCesA*s (Supplemental Table S1). The number of *PtCesA* genes is consistent with that recently reported (Djerbi et al., 2005). The 18 *PtCesA* genes share 54% to 100% protein sequence homology with each other (Supplemental Table S2). Phylogenetically, they form nine groups, eight of which contain a pair of *CesA* genes with a nearly identical sequence (Fig. 1; Supplemental Table S2). In Arabidopsis, there are at least 10 *CesA* genes, which are widely recognized as *AtCesA1* to *10* (http://cellwall.stanford.edu; Delmer, 1999; Richmond and Somerville, 2000; Aspeborg et al., 2005). The 18 *PtCesA* genes share 55% to 88% protein sequence homology with the 10 *AtCesA* genes (Supplemental Table S2). To be consistent with the currently accepted numbering system for the Arabidopsis *CesA* genes, the 18 *PtCesA* genes were named *PtCesA1* to *18*, with *PtCesA1* to *10* being the most closely related homologs of *AtCesA1* to *10*, respectively (Supplemental Fig. S1). *PtCesA11* and *PtCesA1* have an identical sequence, and *PtCesA12* to *18* are the other homologs of *AtCesA1* to *10* (Fig. 1; Supplemental Fig. S1). For *P. trichocarpa*, the eight *PtCesA* pairs are: *PtCesA1(11)/PtCesA10*, *2/5*, *3/13*, *6/9*, *7/17*, *8/18*, *12/14*, and *15/16* (Fig. 1). *PtCesA4* is unique and not paired (Fig. 1; Djerbi et al., 2005) and shares approximately 65% protein sequence homology with all the other *PtCesA*s (Supplemental Table S2). It shares, however, 81%

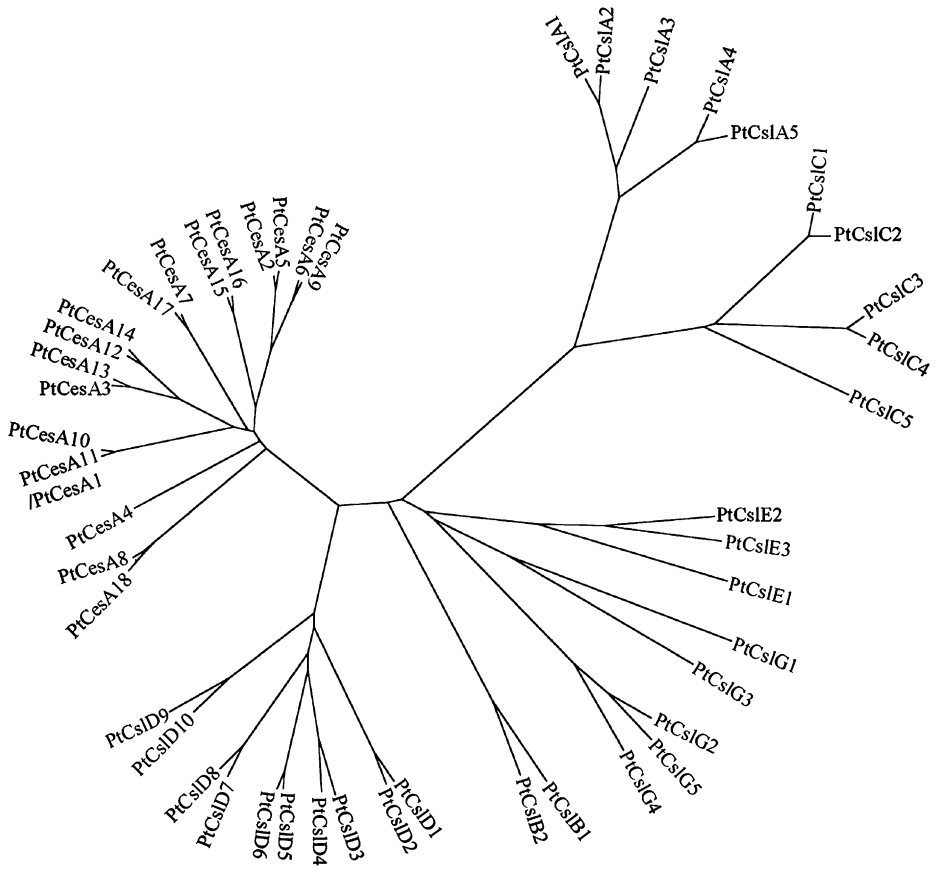

Figure 1. Unrooted dendrogram of 48 *CesA* and *Csl* superfamily gene members in *P. trichocarpa*. The dendrogram was created using the distance matrix of the predicted protein sequences for these 48 *PtCesA* and *PtCsl* genes by the ClustalW multiple sequence alignment program (Thompson et al., 1994) with the default parameter setting.

protein sequence homology with the Arabidopsis *AtCesA4*. *P. trichocarpa* and Arabidopsis *CesA* genes can be classified into seven clades (Supplemental Fig. S1). With the exception of clade VI, which does not contain the *AtCesA* gene, the other six include *CesA* genes from both species.

The remaining 30 of the 48 identified genes belong to the *Csl* gene families and are denoted as *PtCsl*s (Supplemental Table S1). They could be classified into *PtCslA*, *B*, *C*, *D*, *E*, and *G* subfamilies (Fig. 1) according to their protein sequence homology with the 29 known *AtCsl* members that define these subfamilies (http://cellwall.stanford.edu; Richmond and Somerville, 2000). *CslF*, *H*, and *J* subfamilies, which are believed to be monocot-related *Csl*s (Burton et al., 2006; Farrokhi et al., 2006), are absent from the *P. trichocarpa* and Arabidopsis genomes. Although these two genomes share the same, more dicot-specific *Csl* subfamilies, the numbers of the members in many subfamilies differ between these two species. The *P. trichocarpa* genome has fewer *CslA*, *CslB*, and *CslC* members but more *CslD* members than does the Arabidopsis genome. We also found 15 additional *P. trichocarpa* gene models that have partial coding sequences with varying degrees of homology with those of the Arabidopsis *CslC*, *D*, and *G* subfamily genes (Supplemental Table S1). These potential *Csl* genes are, however, not considered as the *Csl* members in this study because of a lack of the full coding sequences in the current gene models. The identities of these 15 genes need to be verified.

Expression Profiling of *P. trichocarpa CesA* and *Csl* Genes

To identify xylem-related *PtCesA* and *PtCsl* genes, we profiled the expression of all possible cellulose synthase superfamily genes in various tissues of *P. trichocarpa* by quantitative real-time PCR. To ensure the transcript amplification is specific, each set of PCR primers was designed so that their sequences would match perfectly with the target sequence but differ in at least three nucleotides from the sequences of all the other superfamily members (Supplemental Table S3). The amplification specificity was further validated based on the generation of a single PCR product from each set of primers and that distinct dissociation curves were derived from the paired *PtCesA*s. We also used pure plasmid DNAs from seven *PtCesA* and *PtCsl* cDNA clones (see "Materials and Methods" for details) as the transcript expression standards in tissues examined. Together, these allowed us to determine the absolute transcript abundance quantified based on the transcript copy numbers for each member in a unit weight of the total RNA. Thus, our approach enabled comparison of the expression of all

the superfamily members in different tissues. The tissues studied here were all from trees under normal growth in a greenhouse.

Of the 48 identified cellulose synthase superfamily genes, 37 were found expressed in the tested tissues (Table I), having transcript copy numbers ranging from approximately 10^3 to $10^7/\mu g$ total RNA. For *CesA* genes, *PtCesA13* and *PtCesA18* were found most highly expressed in the developing xylem, with numbers of transcript molecules being up to approximately 10^4 times that in the other tested tissues. *PtCesA18* is most homologous to a *Populus tremuloides CesA* characterized previously as a xylem-specific cellulose synthase gene (Wu et al., 2000). *PtCesA4*, *5*, *7*, *8*, and *17* also are clearly xylem specific, even though their transcript abundances in xylem and in the other tested tissues were lower than *PtCesA13* and *PtCesA18* (Table I). Other than these seven xylem-specific *CesA* genes, the rest of the *PtCesA* genes (a total of eight) having detectable transcript molecules did not exhibit clear tissue specificity. Transcripts of *PtCesA3*, *PtCesA12*, and *PtCesA15* were either undetectable or essentially absent in the tested tissues. It is possible that these genes may be expressed only in a tissue- or cell-specific manner or under specific growth conditions. Among all the tested tissues, leaves in general had the lowest transcript level for all of the detectable *PtCesA* genes, consistent with the presence of only a small amount of the cellulose-enriched vascular systems in leaves.

The transcripts of 21 of the 30 *PtCsl* genes were detected in the tissues examined (Table I). Overall, the transcript abundance of *Csl* genes is lower than that of *CesA* genes, as observed previously for the Arabidopsis *Csl* genes (Hamann et al., 2004). *PtCslA1*, *A2*, *A5*, and *D6* showed a strong preferential expression in the developing xylem, while *PtCslC1* and *C4* displayed a shoot-tip specificity. No tissue specificity was evident for the remaining 15 detected *PtCsl* genes (Table I) or

Table I. *Transcript copy numbers ($\times 10^4$/mg total RNA) of cellulose synthase superfamily gene members in various P. trichocarpa tissues*

Values are means ± SD of at least three independent PCR runs (see "Materials and Methods" for detailed RNA isolation and PCR primer design and reactions).

Gene Name	Tissues			
	Leaf	Shoot Tip	Phloem	Xylem
PtCesA1/PtCesA11	67.1 ± 0.49	307.1 ± 9.29	155.0 ± 7.01	61.9 ± 0.27
PtCesA2	7.8 ± 1.41	42.9 ± 2.92	57.6 ± 0.93	36.5 ± 1.65
PtCesA4	1.1 ± 0.12	9.52 ± 1.17	7.5 ± 1.20	33.5 ± 1.38
PtCesA5	19.7 ± 2.01	82.3 ± 4.46	56.6 ± 0.89	148.1 ± 8.08
PtCesA6	6.7 ± 0.74	43.9 ± 2.16	16.4 ± 2.20	25.0 ± 1.59
PtCesA7	3.9 ± 0.24	14.6 ± 1.21	16.4 ± 0.17	249.0 ± 33.71
PtCesA8	2.8 ± 0.94	22.7 ± 3.83	18.3 ± 0.69	378.0 ± 20.86
PtCesA9	87.4 ± 1.10	237.0 ± 19.21	169.1 ± 26.30	231.1 ± 19.91
PtCesA10	82.4 ± 10.81	351.1 ± 20.31	123.1 ± 5.45	577.1 ± 40.11
PtCesA12	1.3 ± 0.11	3.3 ± 0.32	3.3 ± 0.85	11.1 ± 0.92
PtCesA13	41.8 ± 3.20	133.0 ± 2.43	73.6 ± 2.85	1080.1 ± 323.1
PtCesA14	53.6 ± 14.51	47.4 ± 1.96	27.9 ± 0.55	60.0 ± 19.9
PtCesA16	31.1 ± 2.05	80.3 ± 3.21	53.4 ± 0.57	27.9 ± 5.27
PtCesA17	1.7 ± 0.44	5.17 ± 0.55	5.9 ± 0.38	115.0 ± 8.06
PtCesA18	7.8 ± 0.84	56.2 ± 10.51	38.9 ± 1.04	1090.0 ± 347.01
PtCslA1	17.7 ± 5.35	12.1 ± 0.31	8.32 ± 1.87	196.1 ± 4.02
PtCslA2	4.06 ± 0.59	18.0 ± 2.12	6.0 ± 1.32	190.1 ± 37.81
PtCslA3	10.0 ± 0.85	28.2 ± 3.88	13.0 ± 0.80	28.5 ± 14.01
PtCslA5	60.9 ± 11.61	179.0 ± 16.21	94.2 ± 8.99	331.1 ± 37.40
PtCslC1	16.2 ± 2.97	102.1 ± 10.01	21.0 ± 1.28	20.3 ± 4.19
PtCslC2	13.9 ± 0.35	24.2 ± 1.48	8.9 ± 0.09	21.7 ± 7.54
PtCslC3	10.8 ± 0.42	18.5 ± 1.19	7.49 ± 1.65	3.18 ± 0.68
PtCslC4	9.8 ± 0.94	42.4 ± 5.86	9.67 ± 1.36	13.4 ± 3.02
PtCslC5	8.8 ± 0.63	16.9 ± 4.19	8.2 ± 1.23	14.0 ± 3.07
PtCslD1	2.5 ± 0.62	2.7 ± 0.58	3.1 ± 0.96	1.41 ± 0.29
PtCslD2	4.5 ± 0.50	5.9 ± 0.41	7.2 ± 0.16	15.7 ± 1.20
PtCslD4	2.1 ± 0.11	4.6 ± 0.70	2.7 ± 0.17	1.5 ± 0.47
PtCslD6	14.6 ± 1.54	60.9 ± 0.82	41.7 ± 0.82	177.1 ± 4.36
PtCslD8	10.1 ± 2.15	4.63 ± 1.43	2.25 ± 0.31	0.69 ± 0.39
PtCslD9	2.9 ± 0.91	2.8 ± 0.28	1.3 ± 0.13	0.2 ± 0.09
PtCslD10	7.4 ± 0.86	7.9 ± 0.66	1.7 ± 0.19	2.9 ± 0.39
PtCslE1	4.6 ± 0.03	2.9 ± 0.50	0.7 ± 0.03	1.9 ± 0.84
PtCslE2	2.6 ± 0.35	0.4 ± 0.03	3.9 ± 0.35	1.2 ± 0.12
PtCslE3	9.1 ± 0.19	7.2 ± 1.38	0.3 ± 0.08	1.8 ± 0.93
PtCslG4	9.3 ± 3.30	5.9 ± 0.33	3.8 ± 0.74	3.6 ± 0.20
PtCslG5	4.8 ± 0.42	9.6 ± 0.31	8.2 ± 0.24	0.9 ± 0.41

for the potential *PtCsl* genes represented by the 15 short gene models (Supplemental Table S4).

Enzymatic Activities of Plant Protein Extracts for the Synthesis of Hemicelluloses

The more xylem-specific expression of several *PtCesA* and *PtCsl* member genes may suggest their involvement in the biosynthesis of wood cellulose and hemicelluloses. Because the lack of a reliable method for determining the biochemical activities of cellulose synthase gene products (Doblin et al., 2002; Peng et al., 2002), we focused on the biochemical functions of *PtCsl* genes. We first investigated the enzymatic activities for the biosynthesis of the hemicellulose backbones in tissues where the expression of *PtCsl*s has been quantified (Table I). GDP-[U-^{14}C]Man, GDP-[U-^{14}C]Glc, and UDP-[U-^{14}C]Xyl, which supply the possible backbone monomers of major wood hemicelluloses, were used as the substrates. Total crude protein was extracted from the young shoot, leaf, developing xylem, and phloem tissues (see "Materials and Methods" for details). Each crude extract preparation was separated into soluble and microsomal fractions, which were analyzed separately for the catalytic activities with these three substrates. The incorporation of radioactivity into the 70% ethanol-insoluble polymeric product was quantified as the enzyme activity. As expected, enzyme activities could not be detected in soluble protein preparations. In contrast, microsomal fractions from the developing xylem displayed strong activities with these three substrates, with UDP-[U-^{14}C]Xyl and GDP-[U-^{14}C]Man being the better substrates than GDP-[U-^{14}C]Glc (Fig. 2). These activities in the microsomes from the other tested tissues were low or negligible (Fig. 2). These results

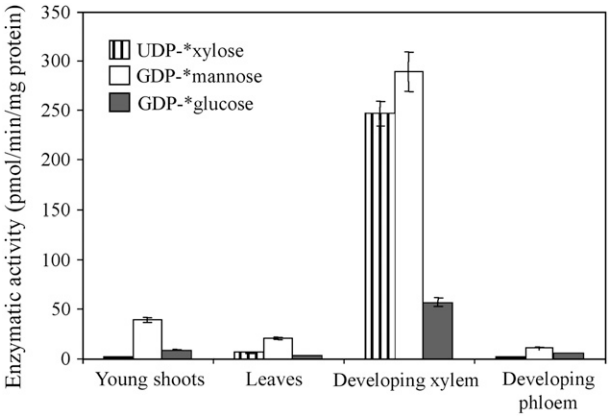

Figure 2. Enzymatic activities of the microsomal fractions from various *P. trichocarpa* tissues for the synthesis of hemicelluloses. The microsomal proteins were isolated from the tested tissues, as indicated, for their enzymatic activities with UDP-[U-^{14}C]Xyl, GDP-[U-^{14}C]Man, and GDP-[U-^{14}C]Glc that would supply the monomeric sugars for the synthesis of xylan and glucomannan backbones. *, Universal ^{14}C labeling. Strong, putative xylan, mannan, and glucan synthase activities were detected in only the developing xylem tissue.

verified the presence in the developing xylem of enzymes converting these monosaccharides into polymers, possibly xylan and glucomannan. These wood hemicellulose activities are likely encoded by the xylem-specific *PtCsl* genes. We then focused on the *PtCslA* family, which as a whole has the most conspicuous xylem specificity (Table I). *CslA* family members were shown to encode ManS or GlcManS activities (Dhugga et al., 2004; Liepman et al., 2005).

Cloning of *PtCslA* Genes and Expression in Drosophila S2 Cells

There are five members in the *PtCslA* subfamily, *PtCslA1* to *5*. We conducted a phylogenetic analysis of *CslA* members from *P. trichocarpa*, Arabidopsis, and rice, and of a *CslA*, *CtManS*, from guar (Dhugga et al., 2004). Except for PtCslA3 and AtCslA9, which are grouped together, the other CslA members are grouped in a more species-specific manner (Fig. 3). This suggests that plant CslA members may exhibit species-specific biochemical functions. The five PtCslA members are divided into three subgroups, with PtCslA1 and PtCslA2 (94% sequence homology) being in one subgroup and PtCslA4 and PtCslA5 (93% homology) in another (Fig. 1). We selected *PtCslA1*, *PtCslA3*, and *PtCslA5*, one member from each of the three subgroups in the *PtCslA* subfamily, for cloning and functional analysis. Based on the predicted transcript sequences, we designed PCR primers to amplify a *P. trichocarpa* xylem cDNA library and identified several full and partial *PtCslA* cDNA coding sequences. Further cloning resulted in the isolation of three full coding sequences, which matched with the predicted transcripts of *PtCslA1*, *PtCslA3*, and *PtCslA5* genes encoding predicted protein sequences of 522, 533, and 538 amino acids, respectively. These protein sequences all contain the conserved motifs characteristic of the processive GTs (Saxena et al., 1995, 2001). These proteins share 71% to 79% sequence homology with each other, 66% to 71% with CtManS (Dhugga et al., 2004), and 71% to 83% with the Arabidopsis AtCslA9, a ManS (Liepman et al., 2005). Using gene-specific sequences in the 5′-untranslated region (UTR) as probes, we carried out northern-blot analysis of the transcript levels of these three *PtCslA* genes in various *P. trichocarpa* tissues and confirmed a keen xylem specificity for *PtCslA1* (Fig. 4). The expression of *PtCslA3* and *PtCslA5* in xylem could not be detected on a northern blot but was conspicuous for *PtCslA*5 in the other vascular system-containing tissues examined. Overall, these northern results are consistent with the transcript copy numbers determined by the real-time PCR (Table I).

To characterize the biochemical function of *PtCslA1*, *PtCslA3*, and *PtCslA5* genes, we constructed the V5-tagged open reading frame (ORF) transgene for each of these genes and a *LacZ* as control and expressed them in Drosophila S2 cells using a pCoBlast vector system (Liepman et al., 2005). After these cells

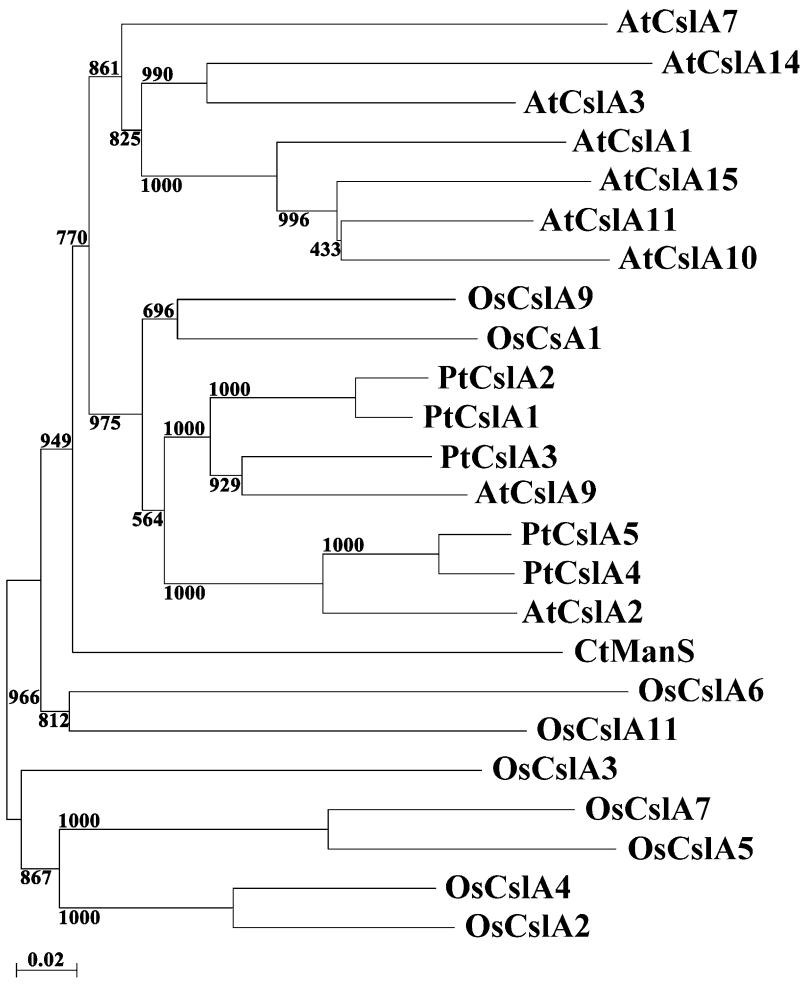

Figure 3. Cladogram of CslA subfamily members of *P. trichocarpa*, Arabidopsis, rice, and guar. The neighbor-joining tree was generated based on the ClustalW protein sequence alignment result using the default setting (Thompson et al., 1994). The bootstrap values were generated based on 1,000 bootstrap trials. Protein sequences of Arabidopsis CslA family members (ATCslAs) were obtained from TAIR (http://www.arabidopsis.org) and rice CslA members (OsCslAs) from the GenBank based on the annotation of the TIGR rice genome annotation project (http://www.tigr.org/tdb/e2k1/osa1/). GenBank accession numbers for ATCslAs and OsCslAs are shown in the parentheses: AtCslA1 (NP_193392.2), AtCslA2 (NP_197666.1), AtCslA3 (NP_850952.1), AtCslA7 (NP_565813.1), AtCslA9 (NP_195996.1), AtCslA10 (NP_173818.1), AtCslA11 (NP_197123.3), AtCslA14 (NP_191159.2), AtCslA15 (NP_193077.2), OsCslA1 (BAD34025), OsCslA2 (AAK98678), OsCslA3 (BAD37274), OsCslA4 (AAL84294), OsCslA5 (AAL82530), OsCslA6 (AAL25127), OsCslA7 (BAC79726), OsCslA9 (BAD37742), OsCslA11 (BAD09847), and CtManS (AAR23313).

were transfected with the expression construct, the stably transformed cell lines were selected and induced by copper sulfate for recombinant protein production. Contents from the whole cell lysates, supernatant after ultracentrifugation, and microsomal fraction were analyzed by western blotting using anti-V5-HRP antibodies as the probe. As shown in Figure 5, the recombinant proteins from all three *PtCslA* genes were expressed in the microsomal fraction. The V5-tagged PtCslA fusion proteins migrated on the protein gel more rapidly than expected, which also was observed for Arabidopsis Csl fusion proteins produced in the S2 cells (Liepman et al., 2005).

Catalytic Activities of the Recombinant Proteins

Microsomal preparations from the S2 cells that produce the three PtCslA and the LacZ recombinant proteins were tested for the catalytic activity with GDP-[U-^{14}C]Man, GDP-[U-^{14}C]Glc, UDP-[U-^{14}C]Xyl, or the mixture of GDP-Man and GDP-Glc with one being U-^{14}C-labeled at the monosaccharide. The concentration and radioactivity for each individual nucleotide sugar used were the same in either the single or mixed substrate cases (Fig. 6). None of these PtCslA recombinant proteins could mediate the conversion of UDP-[U-^{14}C]Xyl. PtCslA1 exhibited a strong activity converting GDP-[U-^{14}C]Man into 70% ethanol-insoluble, radioactive polymeric products, suggesting a possible ManS function for PtCslA1. PtCslA3 recombinant protein also had such activity. Having only a background activity with GDP-[U-^{14}C]Man as the control LacZ protein, PtCslA5 may not be a ManS.

PtCslA1 also utilized GDP-[U-^{14}C]Glc but preferred GDP-[U-^{14}C]Man. PtCslA3 and PtCslA5 had essentially no such activity. Furthermore, PtCslA1 was the only one of these three CslAs exhibiting conspicuous activity capable of converting GDP-[U-^{14}C]Man and GDP-Glc into an ethanol-insoluble polymeric product. This product is likely a [U-^{14}C]Man-labeled glucomannan whose radioactivity was diluted, as compared to the radioactivity in the product from GDP-[U-^{14}C]Man alone, due the incorporation of the nonradioactive Glc residues. Similarly, a [U-^{14}C]Glc-labeled glucomannan was the probable product of PtCslA1-mediated conversion of a mixture of GDP-Man and GDP-[U-^{14}C]Glc. These results are consistent with those of the reactions mediated by the Arabidopsis

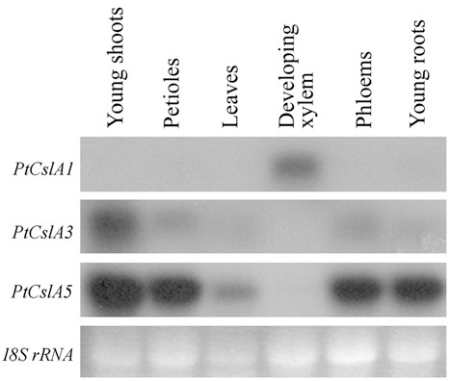

Figure 4. Northern-blotting analysis of *PtCslA1*, *PtCslA3*, and *PtCslA5* gene expression in various *P. trichocarpa* tissues. Total RNA samples were isolated from six tissues as shown. RNA loading levels are indicated by the 18S rRNA transcript signals stained with ethidium bromide. The gene-specific fragments were identified and used as the hybridization probes. *PtCslA1* is expressed specifically in the developing xylem.

AtCslA9 recombinant protein produced by the S2 cells (Liepman et al., 2005). Thus, PtCslA1 also is likely a GlcManS.

Analysis of the PtCslA1-Mediated in Vitro Reaction Products

To further verify the recombinant protein functions, we isolated the in vitro enzyme reaction products and analyzed their composition and linkage types. We focused on the PtCslA1-mediated products from GDP-Man and from mixtures of GDP-Man and GDP-Glc. In vitro polymers produced from the PtCslA1 reaction with GDP-[U-^{14}C]Man were hydrolyzed by trifluoroacetic acid, and the products were added with a mixture of six wood monosaccharides as the elution carrier and separated by HPAEC-PAD HPLC (Wright and Wallis, 1995) and the elution fractions were counted for radioactivity. Only the Man eluents were radioactive (data not shown). This indicates that PtCslA1 is likely a ManS converting Man from GDP-Man into a pure mannan and that the protein preparations from the S2 cells do not epimerize GDP-[U-^{14}C]Man into GDP-[U-^{14}C]Glc. Similarly, analysis of the in vitro polymers from the mixed substrates confirmed the isolation of only radioactive Man from polymers derived from the mixed GDP-[U-^{14}C]Man and GDP-Glc and of exclusively radioactive Glc from the mixed GDP-Man and GDP-[U-^{14}C]Glc substrate pool (data not shown). Thus, PtCslA1 may also possess a GlcManS activity for polymerizing GDP-Man and GDP-Glc into, most likely, a glucomannan.

The in vitro polymers were then hydrolyzed by linkage-specific glycanases: endo-β-D-(1→4)-mannanase, endo-β-D-(1→4)-glucanase (cellulase), and endo-β-D-(1→3)-glucanase (Fig. 7). In the absence of these hydrolytic enzymes (buffer in Fig. 7), essentially no radioactivity could be released into the 70% ethanol solution from the radioactive in vitro polymers. The radioactive polymer from GDP-[U-^{14}C]Man could be effectively digested by endo-β-D-(1→4)-mannanase, releasing over 80% of its radioactivity into solution as mostly monomeric Man units (Wright and Wallis, 1995). The remaining radioactivity was quantitatively retained in the undigested portion of the polymer. However, this GDP-[U-^{14}C]Man-derived polymer could not be hydrolyzed by either endo-β-D-(1→4)- or (1→3)-glucanases, as essentially no radioactivity could be detected in the solution (Fig. 7). The composition and linkage analyses, therefore, point to an in vitro ManS function for PtCslA1 mediating the conversion of GDP-Man into a pure (1→4)-β-D-mannan. The polymer from the mixed GDP-[U-^{14}C]Man and GDP-Glc substrates could also be hydrolyzed by endo-β-D-(1→4)-mannanase with a high efficiency as revealed by the level of the radioactivity in solution (Fig. 7). When this polymer was digested with endo-β-D-(1→4)-glucanase, however, the solution radioactivity decreased drastically, indicative of the polymeric substrate being a [^{14}C]Man-containing glucomannan having strictly β-D-(1→4)-linked Glc residues. Indeed, this polymer could not be digested by endo-β-D-(1→3)-glucanase. The polymer from the substrate pool of GDP-Man and GDP-[U-^{14}C]Glc also responded positively to endo-β-D-(1→4)-mannanase digestion, resulting in a significant release of the radioactivity. Most likely, the radioactivity was derived from the [^{14}C]Glc units that were originally surrounded by Man residues and released after mannanase-mediated hydrolysis of these Man residues. These results also suggest that the oligomeric Glc (or glucan) residues in this polymer are probably infrequent. This is supported by

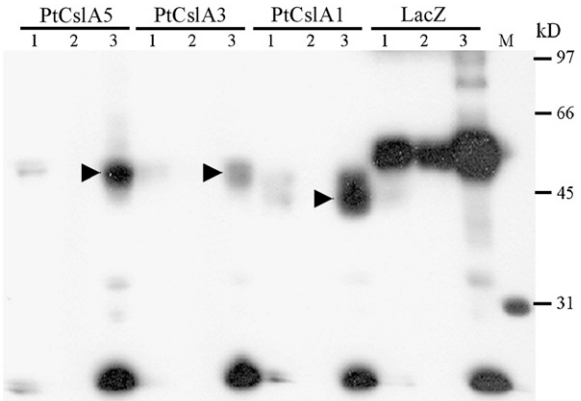

Figure 5. Western-blotting analysis of PtCslA1, PtCslA3, and PtCslA5 recombinant proteins expressed in Drosophila S2 cells. Protein samples (50 μg) from the whole lysates (1), supernatant after ultracentrifugation (2), and microsomal fraction (3) from the S2 cells were separated on SDS-PAGE. LacZ was used as a control. The sizes of the protein markers (M) are indicated. The signals were detected with the antibodies recognizing the V5-tag fused with the recombinant proteins. The expressed PtCslA1, PtCslA3, and PtCslA5 recombinant proteins (marked with arrowheads) were localized in the microsomal fraction (lane 3 in each protein group).

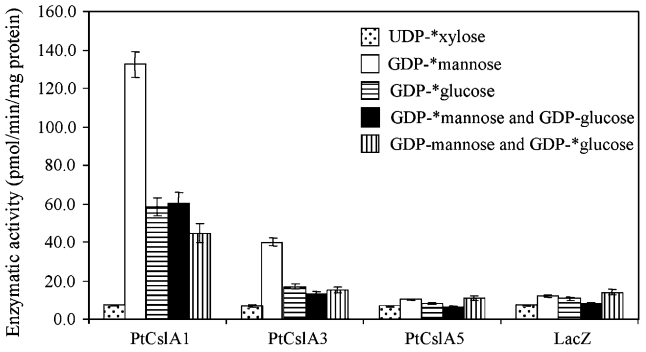

Figure 6. Enzymatic activities of the recombinant proteins from Drosophila S2 cells for the synthesis of hemicelluloses. The microsomal fraction (200~300 μg proteins) of the S2 cells expressing PtCslA1, PtCslA3, PtCslA5, or LacZ protein was incubated with 2 mM GDP-[U-^{14}C]Man (7.722 Bq/nmol), 2 mM GDP-[U-^{14}C]Glc (7.7145 Bq/nmol), 2 mM UDP-[U-^{14}C]Xyl (9.25 Bq/nmol), 2 mM GDP-[U-^{14}C]Man (7.722 Bq/nmol) + 2 mM GDP-Glc, or 2 mM GDP-Man + 2 mM GDP-[U-^{14}C]Glc (7.7145 Bq/nmol). The 70% ethanol-insoluble polymeric product was isolated and counted for the radioactivity for calculating the enzymatic activity as indicated. Values are means ± SDs of at least three independent experiments. None of the recombinant proteins could utilize UDP-Xyl. However, PtCslA1 had putative mannan, glucan, and glucomannan synthase activities, while PtCslA3 exhibited mainly mannan synthase activity. PtCslA5 had essentially no catalytic activities with the substrates tested.

the endo-β-D-(1→4)-glucanase digestion of the polymer that resulted in the release of a low level of radioactivity (Fig. 7). The Glc linkages in this polymer are not the β-D-(1→3) type, as the polymer remained intact after reaction with endo-β-D-(1→3)-glucanase. These polymer linkage analyses further support the composition characterization that the PtCslA1 recombinant protein has a GlcManS activity capable of polymerizing Man from GDP-Man and Glc from GDP-Glc into a (1→4)-β-D-glucomannan.

DISCUSSION

Transcript Abundance Profiling of *PtCesA* and *PtCsl* Genes Identified Xylem-Specific Members in *P. trichocarpa*

We report here a systematic analysis of all the possible cellulose synthase superfamily member genes in a tree species. The identified *PtCesA* genes form several phylogenetic pairs (Fig. 1), an observation being suggested as a result of gene duplication during Populus evolution (Djerbi et al., 2005). However, most of the paired *PtCesA* genes, which presumably have a similar function, have distinguishable tissue expression patterns (Table I). These pairs include *PtCesA1(11)/PtCesA10*, *2/5*, *6/9*, *12/14*, and *15/16*. For example, for the *PtCesA1(11)/10* pair, *PtCesA1(11)* is more shoot-tip specific, whereas *PtCesA10* has a higher xylem specificity. While *PtCesA2* lacks tissue specificity, its paired homolog, *PtCesA5*, is apparently more xylem specific. These results may imply a more tissue- or cell type-specific division of function for the *CesA* genes following their duplication in the *P. trichocarpa* genome.

In contrast to the paired *PtCesA*s having diverged expression patterns, the *PtCesA*s of the *7/17* pair have well-matched expression patterns, as do those of the *8/18* pair (Table I). They are all clearly xylem specific. Notably, *PtCesA4* (another xylem-specific *CesA*), the *PtCesA7/17* pair, and the *PtCesA8/18* pair are the homologs of Arabidopsis *AtCesA4*, *7*, and *8*, respectively. The gene products of these three *AtCesA* genes are known as the set of the three cellulose synthases required for the biosynthesis of cellulose in the secondary cell walls (Taylor et al., 1999, 2000, 2003). The redundant xylem-specific expression of *PtCesA7* and *PtCesA17* and of *PtCesA8* and *PtCesA18* is consistent with the massive production of cellulose in xylem secondary cell walls for wood formation. However, there is another xylem-specific *CesA*, the *PtCesA13*. It is one of the two *PtCesA* genes having the highest transcript level in the developing xylem (Table I). Perhaps more than three *CesA*s or a set of *CesA*s that is different from Arabidopsis are required for the biosynthesis of cellulose in xylem cell walls of *P. trichocarpa*, or of trees in general. Interestingly, while *PtCesA13* has a high transcript abundance in xylem, the transcripts of its paired homolog, *PtCesA3*, were undetectable in all tested tissues. Because all these transcripts were

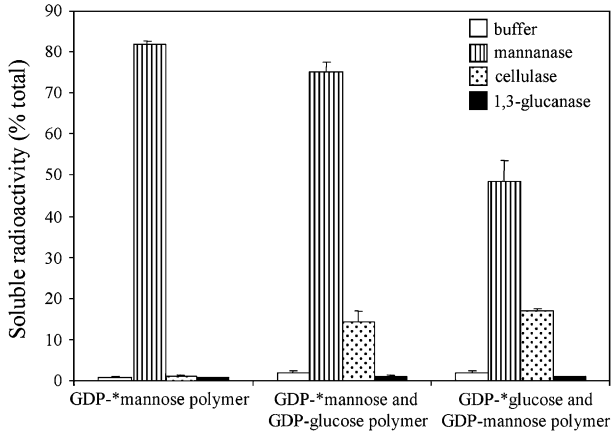

Figure 7. Analysis of the PtCslA1 recombinant protein-mediated in vitro reaction products with linkage-specific glycanases. The 70% ethanol-insoluble polymeric product from PtCslA1-mediated reaction with GDP-[U-^{14}C]Man, GDP-[U-^{14}C]Man + GDP-Glc, or GDP-Man + GDP-[U-^{14}C]Glc was isolated. Each type of reaction product was hydrolyzed by endo-β-D-(1→4)-mannanase (shown as mannanase), endo-β-D-(1→4)-glucanase (cellulase), and endo-β-D-(1→3)-glucanase (1,3-glucanase), respectively. Buffer without any hydrolytic enzyme was used in the control reaction. Values of the ^{14}C radioactivity released from the hydrolysis of the in vitro product as percentage of the original radioactivity incorporated in the in vitro polymer are shown. Values are means ± SDs of at least three independent experiments. The analyses confirmed that the PtCslA1 recombinant protein had a mannan synthase activity capable of polymerizing Man from GDP-Man into a (1→4)-β-D-mannan and a glucomannan synthase activity for polymerizing Man from GDP-Man and Glc from GDP-Glc into a (1→4)-β-D-glucomannan.

analyzed for tissues under normal growth, it is unknown whether the expression of those *PtCesA* genes with undetectable or low transcripts is only inducible under specific growth conditions (Wu et al., 2000). Our transcript analyses provide evidence for growth- or development-regulated transcriptional control of cellulose synthesis in *P. trichocarpa*. The quantitative transcript abundances may help guide further studies to learn about this control.

The transcript levels of a majority of the *PtCsl* genes in the tissues examined were too low to be conclusive about the expression patterns (Table I). The transcripts of only five *Csl* genes, *PtCslA1*, *PtCslA2*, *PtCslA5*, *PtCslC1*, and *PtCslD6*, could be detected at significant levels. In this study, we focused on the *PtCslA* family; the function of *PtCslD6*, the only xylem-specific *PtCsl* gene outside the *PtCslA* family, remains to be characterized.

Putative XylS Activities in Stem-Developing Xylem of *P. trichocarpa*

We detected in the microsomes from the developing xylem strong activities converting UDP-Xyl or GDP-Man into 70% ethanol-insoluble polymers (Fig. 2). However, the similar plant protein activities observed for these two substrates are inconsistent with the fact that the quantity of xylan is normally severalfold higher than that of glucomannan in the angiosperm wood (Timell, 1964, 1969; Fengel and Wegener, 1979, 1984). It is possible that the plant protein reaction products from either substrate are a similar mixture of radioactive xylan and mannan. This assumes the presence of sugar nucleotide exchange reactions that would effectively interconvert UDP-[U-^{14}C]Xyl and GDP-[U-^{14}C]Man. Although this might explain the similar enzyme activities observed, such an epimerization activity has never been reported (Leloir, 1951; Adams, 1976; Dalessandro and Northcote, 1977). Indeed, a radioactive xylan polymer with no incorporation of Man residues was synthesized from UDP-[^{14}C]Xyl by microsome proteins from corn cobs (Bailey and Hassid, 1966), further negating the activities for an interconversion of UDP-Xyl and GDP-Man. The similar UDP-Xyl- and GDP-Man-utilizing activities observed may have other implications. It may suggest that the in vivo xylan synthase activity involves protein partners (Zhong et al., 2005) or other factors (Dhugga, 2005; Liepman et al., 2005) forming an effective machinery for the biosynthesis of xylan. The microsomal protein preparation may have disrupted such machinery, making the in vitro xylan synthase activity far less efficient than its native state. This proposition needs to be validated.

In Vitro Enzymatic Activities of PtCslA Members Are Distinct from Each Other

Based on the sequence-defined subfamily grouping (http://cellwall.stanford.edu; Richmond and Somerville, 2000), there are only three types of members in the *PtCslA* subfamily, represented by *PtCslA1*, *PtCslA3*, and *PtCslA5*, respectively. They share high (71%–79%) protein sequence homology, but their recombinant proteins produced by the S2 cells show distinct catalytic activities. *PtCslA1* and *PtCslA3* encode a ManS activity, whereas PtCslA5 has essentially no such activity (Fig. 6). The in vitro polymer products of the recombinant PtCslA1 with GDP-Man are a pure mannan, suggesting the absence in the system of the epimerization of the three sugar nucleotides that were used as the substrates. These three types of sugars are the possible backbone constituents of the only two significant hemicelluloses known in the angiosperm wood. The fact that none of these sugars can be utilized by PtCslA5, even though a good level of this protein was produced by the S2 cells (Fig. 6), provides in vitro evidence that PtCslA5 may not be associated with the biosynthesis of the two wood hemicelluloses. But remarkably, *PtCslA5* has, among all the detectable *Csl* gene members in *P. trichocarpa*, the highest transcript copy numbers in all tissues tested (Table I). In particular, its expression is more associated with the vascular systems in *P. trichocarpa* (Table I; Fig. 4). Whether PtCslA5 is associated with the biosynthesis of wood hemicelluloses remains to be elucidated. Perhaps roles for *PtCslA5* gene and gene product can be better revealed using the plant systems.

The ManS activity of PtCslA3 recombinant protein is specific for mannan synthesis (Fig. 6). Pure mannan, however, has never been isolated from angiosperm tree species, due probably to its low quantity. This is consistent with the low levels of *PtCslA3* transcripts in all tissues tested (Table I). It is possible that the low level of mannan may act as signaling molecules (Liepman et al., 2005) instead of a structure polysaccharide. Indeed, complex polysaccharides have numerous biological, including signaling and growth-regulating, properties (Creelman and Mullet, 1997).

Recombinant protein activity assays and in vitro product characterizations validated that, of all the three *PtCslA* gene types, *PtCslA1* represents the most conspicuous one that encodes both ManS and GlcManS activities capable of mediating the synthesis of (1→4)-β-D-mannan and (1→4)-β-D-glucomannan (Figs. 6 and 7). These in vitro functions are similar to those of the Arabidopsis AtCslA9 (Liepman et al., 2005), which shares 80% sequence homology with PtCslA1.

Surprisingly, AtCslA9 and PtCslA3 share higher sequence homology at 83%, but PtCslA3 does not have in vitro GlcManS activities (Fig. 6). PtCslA3 acts instead more like the Arabidopsis AtCslA7 (Liepman et al., 2005) and both are more of a ManS. These two proteins having a seemingly similar function share, however, only 60% sequence homology. More intriguingly, Arabidopsis AtCslA2 and PtCslA5 share 84% sequence homology, but AtCslA2 is a ManS and also is likely a GlcManS (Liepman et al., 2005), whereas PtCslA5 is neither a ManS nor a GlcManS (Fig. 6). Evidently, sequence homology of proteins between

species may not be a general indicator for functional similarity. This may be a consequence of gene function divergence following speciation. In addition, the numbers of the members in certain *Csl* subfamilies, including the *CslA* subfamily, differ between *P. trichocarpa* and Arabidopsis (see "Results"). These variations in gene function and diversification may reflect the requirement of different types and quantities of the hemicelluloses by herbaceous and by woody dicots. In *P. trichocarpa*, all the three possible types of *CslA* genes are more vascular tissue specific, but likely only one is required for the synthesis of wood glucomannan.

PtCslA1 Likely Encodes a Key GlcManS for the Synthesis of Wood Glucomannan

Although *PtCslA1* encodes an in vitro ManS activity, the presence of pure mannan in wood of angiosperm trees has not been demonstrated, to our knowledge. But glucomannan, or (1→4)-β-D-glucomannan, can be readily purified from angiosperm wood. (1→4)-β-D-Glucomannan does not contain long stretches of mannan or glucan residues. Instead, it has alternated Man and Glc residues with Glc:Man ratios of 1:1 to 1:3 (Timell, 1986; Jacobs et al., 2002). This alternated polymerization of Man and Glc in glucomannan synthesis was also projected by the radioactivity products after enzymatic hydrolysis of the in vitro glucomannan (Fig. 7). Thus, the observed in vitro "mannan" and "glucan" synthesis functions for PtCslA1 recombinant protein may not be important for the biosynthesis of glucomannan in vivo. The in vivo function of PtCslA1 may simply be that of a GlcManS for the synthesis of one of the two important structure hemicelluloses in the angiosperm wood. This proposition is in line with the devoted expression of *PtCslA1* in the secondary xylem (Fig. 4; Table I), the main tissue type where glucomannan deposits. Furthermore, based on the incorporation (Fig. 6) and release (Fig. 7) of the radioactive Glc and Man units, the Glc:Man ratio in the in vitro (1→4)-β-D-glucomannan was estimated to be approximately 1:2 to 1:3, consistent with the structure of angiosperm wood's glucomannan.

Glucomannan is a minor but significant component in angiosperm wood. In contrast, in conifer wood, glucomannan, which is slightly branched with Gal residues, is the predominant hemicellulose (Timell, 1986; Jacobs et al., 2002). The exact physiological function of glucomannan in trees is not clear. However, glucomannan is a highly undesirable trait in conifer wood for pulp and paper production. Nearly 60% of all pulp produced in the United States is manufactured from conifers, and lower limits on chemical/energy intensities for pulp production from these species have been reached (Nilsson et al., 1995). During pulping of conifer wood, glucomannan (approximately 20% of the wood weight) is almost completely degraded at the onset of the process, consuming approximately 25% of the chemicals intended to remove lignin to produce woodpulp (Rydholm, 1965; Gellerstedt, 2001). Thus, engineered conifers with less glucomannan are expected to drastically lower the chemical intensity limits for pulp production. As energy feedstock, on the other hand, wood modified for an increased quantity of glucomannan, the six-carbon sugar pool, would be highly desirable for improved ethanol yield. The identification of genes encoding ManS and GlcManS by the previous and current studies may help facilitate these biotechnological applications to improving the economics of the wood and future wood-based biofuel industries.

MATERIALS AND METHODS

Reagents and Enzymes

GDP-[^{14}C]Man (9.6 GBq/mmol) and UDP-[^{14}C]Xyl (9.8 GBq/mmol) were obtained from Perkin-Elmer, GDP-[^{14}C]Glc (11.1 GBq/mmol) from American Radiolabeled Chemicals, and nonradioactive UDP-Xyl from Carbosource Services. Endo-β-D-(1→4)-mannanase purified from *Bacillus* sp., endo-β-D-(1→4)-glucanase (cellulase) from *Aspergillus niger*, and endo-β-D-(1→3)-glucanase from *Trichoderma* sp. were obtained from Megazyme. Oligonucleotide primers were synthesized by MWG Biotech. Vectors, *Escherichia coli* cells, Drosophila S2 cells, culture media, and anti-V5-HRP antibody were purchased from Invitrogen, SuperSignal West Pico chemiluminescent from Pierce, Bradford protein assay concentrate from Bio-Rad, Immobilon-P membrane from Millipore, α-[^{32}P]dCTP from MP Biomedicals, DECAprime II labeling kit from Ambion, SYBR Green PCR master mix and reverse transcription-PCR kit from Applied Biosystems, RNase-free DNase I from Promega, RNeasy plant RNA isolation kit from Qiagen, and TaKaRa ExTaq polymerase from Takara Bio. All other chemicals were obtained from Sigma-Aldrich or Fisher Scientific.

Sequence Analysis of Cellulose Synthase Superfamily Members

*PtCesA*s and *PtCsl*s were identified by searching through the current release of 58,036 *Populus trichocarpa* gene models (http://www.jgi.doe.gov/poplar/) for genes homologous to the 10 Arabidopsis (*Arabidopsis thaliana*) CesA and 29 Arabidopsis Csl protein sequences with e values less than 1E-05 using the BLASTX program (Altschul et al., 1997). The predicted protein sequences of the BLASTX-identified gene models were further screened for completeness by analyzing their transmembrane domain profiles with TMHMM (http://www.cbs.dtu.dk/services/TMHMM/) and the presence of the conserved motifs that are common to *CesA* and *Csl* genes (Saxena et al., 1995; Saxena and Brown, 1997). Cellulose synthase superfamily members of Arabidopsis and rice (*Oryza sativa*) were obtained from the GenBank based on the annotation of The Arabidopsis Information Resource (TAIR; http://www.arabidopsis.org) and the The Institute for Genomic Research Rice Genome Annotation project (http://www.tigr.org/tdb/e2k1/osa1/). Phylogenetic trees and their associated bootstrap values were analyzed using the ClustalW multiple sequence alignment program (Thompson et al., 1994). The neighbor-joining trees were created based on the distance matrices derived from the results of multiple sequence alignments using the default settings, followed by 1,000 bootstrap trials to evaluate the qualities of the trees.

RNA Isolation and Gel-Blot Analysis

Leaf (from four to six internodes), stem-developing phloem, stem-developing xylem, young shoot tip (one to three internodes), and fine root tissues were harvested from 2-year-old *P. trichocarpa* (Nisqually-1) trees grown in our greenhouse and stored immediately in liquid nitrogen until use. Total RNAs were isolated from these tissues, and the RNA quality was examined by UV spectrogram scan and gel electrophoresis, as we did previously (Lu et al., 2005). The total RNA was used for northern blotting and real-time PCR analysis. RNA gel blotting and hybridization were performed under high stringency conditions (65°C) as described previously (Hu et al., 1999). A 5′-end fragment including the 5′-UTR was selected from each of the three

PtCslA genes (*PtCslA1*, *PtCslA3*, and *PtCslA5*) and labeled with α-[^{32}P]dCTP using a DECAprime II labeling kit and used as the probe for hybridization.

Gene-Specific PCR Primer Design and Real-Time PCR Analysis of Gene Transcript Copy Numbers

Based on the identified *PtCesA* and *PtCsl* gene models, PCR primers were designed so that the sequences of each set of primers would match perfectly with the target *PtCesA* or *PtCsl* sequence but differ in at least three nucleotides from the sequences of all the other superfamily members (Supplemental Table S3). Each designed primer set was expected to amplify a PCR product from a specific exon with a size of approximately 100 bp in length.

Total RNA was treated with RNase-free DNase I and purified by RNeasy plant RNA isolation kit. Total RNA (200 ng) was reverse transcribed using SYBR Green PCR master mix and reverse transcription-PCR kit according to the manufacturer's manual. Real-time PCR was conducted using an Applied Biosystems 7900HT sequence detection system (Shi and Chiang, 2005). For each reaction, the 25-μL mixture contained the first-strand cDNA (equivalent to 100 pg of total RNA), 5 pmol each of the forward and reverse primers, and 12.5 μL of 2$\times$ SYBR Green PCR master mix. The amplification program was as follows: 95°C for 10 min, 40 cycles at 95°C for 15 s, and 60°C for 1 min. After amplification, a thermal denaturing cycle was added to derive the dissociation curve of the PCR product to verify amplification specificity. Each reaction was repeated at least three times.

A formula for quantifying the transcript copy numbers per unit weight of total RNA was derived. Pure plasmid DNAs from seven cDNA clones (*PtCesA10*, *PtCesA18*, *PtCslA1*, *PtCslA3*, *PtCslA5*, *PtCslC1*, and *PtCslC2*; see cDNA cloning below) were used as the standards for establishing a quantitative correlation between the copy numbers of the target transcript molecules in a sample and the Ct values. Based on the known M_r of the plasmid, the transcript copy numbers were calculated from the plasmid concentrations after a serial dilution (0, 10^{-4}, 10^{-3}, 10^{-2}, 10^{-1}, 10^{0}, 10^{1}, and 10^{2} pg/μL). The transcript copy numbers in 10^{-4} pg/μL were in a range of approximately 12 to 18 for these seven plasmid DNAs. A formula from the mean of the standard curves (Ct values versus log[initial transcript copy numbers]) generated from the real-time PCR runs of the seven plasmids was derived (with $R^2 > 0.995$) according to the manufacturer's protocols (ABI Prism 7900HT; Applied Biosystems) and was used to quantify the copy numbers of the target gene transcripts. Thus, copy numbers = $c \times 10^{(b + a \times Ct)}$, where c is determined experimentally as usual, and b is 11.6 $\pm$ 0.05 (mean $\pm$ SE) and a is -0.3 ± 0.004 (mean $\pm$ SE); both were derived for this study based on the standard gene experiments. The PCR amplification efficiencies for all seven of these standard genes were nearly identical, as revealed by the low SE values in the formula. For using this formula, we assumed that the other *PtCesA* and *PtCsl* genes also have the same PCR efficiency as the seven standard genes and the tested cDNAs/RNAs have the same PCR efficiency as the plasmid DNAs at the beginning of the PCR reaction. For each target gene experiment, at least one of the standard genes was included, and the PCR results from these standard genes were highly reproducible, validating the appropriateness of the established formula.

Crude Plant Protein Extraction and Microsomal Protein Preparation from *P. trichocarpa*

The tissue sample (1.5 g) was ground in liquid nitrogen and homogenized at 4°C in 30 mL of extraction buffer: 50 mM HEPES-KOH, pH 7.5, containing 0.4 M Suc, 5 mM $MgCl_2$, 2 mM dithiothreitol (DTT), 1 mM phenylmethylsulfonyl fluoride, 1 mg/L pepstatin A, 1 mg/L leupeptin, and 2% (w/w) Polyclar-AT. The homogenate was centrifuged at 1,000*g* for 15 min at 4°C and filtered with Miracloth. The filtrate was centrifuged at 100,000*g* for 1.5 h to collect the microsomal fractions (Osakabe et al., 1999). The microsomal debris was then resuspended in 0.5 mL of the extraction buffer using a glass homogenizer. Protein concentrations were determined by the Bio-Rad protein assay system.

PtCsl cDNA Cloning and Heterologous Expression in Drosophila S2 Cells

PtCesA1, *PtCesA3*, and *PtCesA5* cDNAs were PCR cloned. Based on the predicted cDNA sequences, gene-specific primer sets (*PtCslA1*: 5′-end primer, ACCATGGTGTTTCCTGCCGGTCGGGATG, and 3′-end primer, AGAGTGGGGGACAAAGGTGC; *PtCslA3*: 5′-end primer, ACCATGGAGAGGCTAACCTCAAC, and 3′-end primer, AGAGCGGGGAACAATGGTGC; *PtCslA5*: 5′-end primer, ACCATGGCTGAAGTTTCGCCGAAA, and 3′-end primer, AATAATGGTACCAACGTATCCAAT; start codons are underlined) were designed to amplify the coding sequences, which were subsequently cloned into pMT/V5-His-TOPO vector. *P. trichocarpa* xylem lambda phage cDNA library was used as the template and ExTaq polymerase was employed to ensure the sequence authenticity of the PCR products. The cDNA clones were purified and verified by full sequencing from both directions. Following this approach, *PtCesA10*, *PtCesA18*, *PtCslC1*, and *PtCslC2* cDNAs were also cloned and sequenced.

Drosophila S2 cells were cotransfected with the pCoBlast vector and the pMT/V5-His-TOPO vector containing the target *PtCslA* ORF (pMT/*lacZ* containing *lacZ* ORF was used as a control for cotransfection) according to manufacturer's protocols. After transfection, stably transformed lines of the S2 cells were selected in Schneider's Drosophila medium containing 25 mg/L blasticidin. Protein expression was induced with the addition of copper sulfate (0.75 mM) for 24 h. The induced cells were harvested by centrifugation at 500*g* for 5 min followed by microsomal protein preparation.

Microsomal Protein Preparation from Drosophila S2 Cells

The S2 cells from 32-mL cultures were harvested and then disrupted by sonication in 7 mL of an extraction buffer (50 mM HEPES-KOH, pH 7.5, containing 0.4 M Suc, 5 mM $MgCl_2$, 2 mM DTT, 1 mM phenylmethylsulfonyl fluoride, 1 mg/L pepstatin A, and 1 mg/L leupeptin) for 2 min at 4°C. The microsomal protein preparation was performed as described above for the plant cells.

Immunoblot Analysis of Recombinant Proteins

Protein preparation (50 μg) was incubated in standard SDS-PAGE buffer for 15 min at 42°C. After separation on SDS-PAGE, proteins were transferred to an Immobilon-P membrane by electroblotting (Li et al., 2001). The membrane was blocked with bovine serum albumin for 1 h at room temperature and treated with anti-V5-HRP antibody overnight at 4°C. The signal was detected by using SuperSignal West Pico chemiluminescent substrate. After detection, the membrane was stained with Coomassie Brilliant Blue R-250 to verify uniform loading and transfer.

Activity Assays for Microsomal Protein Preparations from Plant and S2 Cells

Enzyme assays were performed essentially according to Liepman et al. (2005). Briefly, the assay was carried out in 60 μL of reaction mixture containing assay buffer (50 mM HEPES-KOH, pH 7.5, containing 2.5 mM DTT, 2.5 mM $MgCl_2$, 5 mM $MnCl_2$, and 6% glycerol), microsomal proteins (200–300 μg), and substrate(s). The following substrate concentrations were used. For individual substrate reactions: 2 mM GDP-[U-^{14}C]Man (7.722 Bq/nmol), 2 mM GDP-[U-^{14}C]Glc (7.7145 Bq/nmol), or 2 mM UDP-Xyl (9.25 Bq/nmol). Mixed substrate reactions contained 2 mM GDP-[U-^{14}C]Man (7.722 Bq/nmol) and 2 mM GDP-Glc; 2 mM GDP-Man and 2 mM GDP-[U-^{14}C]Glc (7.7145 Bq/nmol). Reaction mixtures were incubated at 25°C for 30 min, and the reaction was terminated by adding 1 mL of 70% ethanol containing 2 mM EDTA. Carob galactomannan (200 μg) was added as a carrier. Products were precipitated at -20°C and pelleted at 16,000*g* for 10 min. Pellets were washed four times with 70% ethanol containing 2 mM EDTA to remove excess radioactivity. Washed pellet was then resuspended in water and counted using a Beckman Coulter LS 6500 liquid scintillation counter.

Characterization of Polysaccharide Products

The identity of the radioisotope-labeled products was examined by both acid hydrolysis and linkage-specific hydrolase digestion. Product pellet was harvested from large scale of reactions (10-fold scaled up from the normal reaction described above) and washed with 70% ethanol containing 2 mM EDTA as described above and dried. The pellet was hydrolyzed in 0.1 mL of 2 M trifluoroacetic acid at 120°C for 1 h. After addition of a mixture of Ara, Rha, Gal, Glc, Xyl, and Man standards, the hydrolysates were filtered and subjected (20 μL) to an anion-exchange chromatography (Dionex) consisting of an AS50 autosampler, a GP40 gradient pump, a CarboPac PA1 column, and an ED40

electrochemical detector using water as the eluent at a flow rate of 1.2 mL min^{-1}. Before each sample injection, the column was washed and equilibrated with 200 mN NaOH for 20 min, with 400 mN NaOH as the post column mobile phase at a flow rate of 0.15 mL min^{-1}. The system afforded a well separation and detection of the six sugars. The eluents corresponding to each sugar were collected and counted (Beckman Coulter LS 6500).

For hydrolase digestions, manufacturer's protocols were followed. The in vitro product pellet was resuspended in 150 μL of buffer [0.1 M Gly-NaOH, pH 8.8, for endo-β-D-(1→4)-mannanase, 0.1 M AcONa-AcOH, pH 4.5, for endo-cellulase, and 0.1 M AcONa-AcOH, pH 4.0, for endo-β-D-(1→3)-glucanase] and hydrolyzed with 10 mU of the hydrolytic enzyme for 1 h at 40°C. After hydrolysis, 1.3 mL of 70% ethanol containing 2 mM EDTA and 200 μg carob galactomannan were added to the reaction mixture, which was precipitated at −20°C for 1 h and pelleted at 16,000*g* for 10 min. The radioactivities of the supernatant and pellet were counted (Beckman Coulter LS 6500) separately.

Supplemental Data

The following materials are available in the online version of this article.

Supplemental Figure S1. Cladogram of the *CesA* genes from Arabidopsis and poplar genomes.

Supplemental Table S1. The gene *loci* of *PtCesA* and *PtCsl* members.

Supplemental Table S2. *CesA* sequence homology between Arabidopsis and *P. trichocarpa*.

Supplemental Table S3. List of real-time PCR primers.

Supplemental Table S4. Transcript copy numbers of the partial putative *PtCsl* genes.

ACKNOWLEDGMENTS

We thank Prof. Hou-min Chang (North Carolina State University) and our lab members, Dr. Rui Katahira and Dr. Ting-Feng Yeh, for their assistance on the use of the Dionex anion-exchange chromatography for sugar analysis. We are grateful for the sequence information produced by the U.S. Department of Energy Joint Genome Institute (http://www.jgi.doe.gov).

Received July 12, 2006; accepted August 28, 2006; published September 1, 2006.

LITERATURE CITED

Adams E (1976) Catalytic aspects of enzymatic racemization. Adv Enzymol Relat Areas Mol Biol **44:** 69–138

Altschul SF, Madden TL, Schäffer AA, Zhang J, Zhang Z, Miller W, Lipman DJ (1997) Gapped BLAST and PSI-BLAST: a new generation of protein database search programs. Nucleic Acids Res **25:** 3389–3402

Aspeborg H, Schrader J, Coutinho PM, Stam M, Kallas A, Djerbi S, Nilsson P, Denman S, Amini B, Sterky F, et al (2005) Carbohydrate-active enzymes involved in the secondary cell wall biogenesis in hybrid aspen. Plant Physiol **137:** 983–997

Bailey RW, Hassid WZ (1966) Xylan synthesis from uridine-diphosphate-D-xylose by particulate preparations from immature corncobs. Proc Natl Acad Sci USA **56:** 1586–1593

Brown RM Jr, Montezinos D (1976) Cellulose microfibrils: visualization of biosynthetic and orienting complexes in association with the plasma membrane. Proc Natl Acad Sci USA **73:** 143–147

Burton RA, Wilson SM, Hrmova M, Harvey AJ, Shirley NJ, Medhurst A, Stone BA, Newbigin EJ, Bacic A, Fincher GB (2006) Cellulose synthase-like *CslF* genes mediate the synthesis of cell wall (1,3;1,4)-β-D-glucans. Science **311:** 1940–1942

Campbell JA, Davies GJ, Bulone V, Henrissat B (1997) A classification of nucleotide-diphospho-sugar glycosyltransferases based on amino acid sequence similarities. Biochem J **326:** 929–939

Carpita N, McCann M (2000) The cell wall. *In* BB Buchana, W Gruissem, RL Jones, eds, Biochemistry and Molecular Biology of Plants. American Society of Plant Biologists, Rockville, MD, pp 52–108

Coutinho PM, Deleury E, Henrissat B (2003) The families of carbohydrate-active enzymes in the genomic era. J Appl Glycosci (1999) **50:** 241–244

Creelman RA, Mullet JE (1997) Oligosaccharins, brassinolides, and jasmonates: nontraditional regulators of plant growth, development, and gene expression. Plant Cell **9:** 1211–1223

Cutler S, Somerville C (1997) Cloning in silico. Curr Biol **7:** R108–R111

Dalessandro G, Northcote DH (1977) Changes in enzymic activities of nucleoside diphosphate sugar interconversions during differentiation of cambium to xylem in pine and fir. Biochem J **162:** 281–288

Delmer DP (1999) Cellulose biosynthesis: exciting times for a difficult field of study. Annu Rev Plant Physiol Plant Mol Biol **50:** 245–276

Dhugga KS (2001) Building the wall: genes and enzyme complexes for polysaccharide synthases. Curr Opin Plant Biol **4:** 488–493

Dhugga KS (2005) Plant Golgi cell wall synthesis: from genes to enzyme activities. Proc Natl Acad Sci USA **102:** 1815–1816

Dhugga KS, Barreiro R, Whitten B, Stecca K, Hazebroek J, Randhawa GS, Dolan M, Kinney AJ, Tomes D, Nichols S, et al (2004) Guar seed β-mannan synthase is a member of the cellulose synthase super gene family. Science **303:** 363–366

Djerbi S, Lindskog M, Arvestad L, Sterky F, Teeri TT (2005) The genome sequence of black cottonwood (*Populus trichocarpa*) reveals 18 conserved cellulose synthase (CesA) genes. Planta **221:** 739–746

Doblin MS, Kurek I, Jacob-Wilk D, Delmer DP (2002) Cellulose biosynthesis in plants: from genes to rosettes. Plant Cell Physiol **43:** 1407–1420

Edwards ME, Dickson CA, Chengappa S, Sidebottom C, Gidley MJ, Reid JSG (1999) Molecular characterization of a membrane-bound galactosyltransferase of plant cell wall matrix polysaccharide biosynthesis. Plant J **19:** 691–697

Faik A, Price NJ, Raikhel NV, Keegstra K (2002) An Arabidopsis gene encoding an α-xylosyltransferase involved in xyloglucan biosynthesis. Proc Natl Acad Sci USA **99:** 7797–7802

Farrokhi N, Burton RA, Brownfield L, Hrmova M, Wilson SM, Bacic A, Fincher GB (2006) Plant cell wall biosynthesis: genetic, biochemical and functional genomics approaches to the identification of key genes. Plant Biotechnol J **4:** 145–167

Fengel D, Wegener G (1979) Hydrolysis of polysaccharides with trifluoroacetic acid and its application to rapid wood and pulp analysis. *In* RM Brown Jr, L Jurasek, eds, Hydrolysis of Cellulose: Mechanisms of Enzymatic and Acid Catalysis. Advances in Chemistry Series No. 181. ACS, Appleton, WI, pp 145–158

Fengel D, Wegener G (1984) Chemical composition and analysis of wood. *In* Wood: Chemistry, Ultrastructure, Reactions. Walter de Gruyter, Berlin, pp 26–65

Gardiner JC, Taylor NG, Turner SR (2003) Control of cellulose synthase complex localization in developing xylem. Plant Cell **15:** 1740–1748

Geisler-Lee J, Geisler M, Coutinho PM, Segerman B, Nishikubo N, Takahashi J, Aspeborg H, Djerbi S, Master E, Andersson-Gunneras S, et al (2006) Poplar carbohydrate-active enzymes. Gene identification and expression analyses. Plant Physiol **140:** 946–962

Gellerstedt G (2001) Pulping chemistry. *In* DS-N Hon, N Shiraishi, eds, Wood and Cellulose Chemistry, Ed 2. Marcel Dekker, New York, pp 859–905

Girke T, Lauricha J, Tran H, Keegstra K, Raikhel N (2004) The Cell Wall Navigator Database. A systems-based approach to organism-unrestricted mining of protein families involved in cell wall metabolism. Plant Physiol **136:** 3003–3008

Hamann T, Osborne E, Youngs HL, Misson J, Nussaume L, Somerville C (2004) Global expression analysis of CESA and CSL genes in Arabidopsis. Cellulose **11:** 279–286

Hazen SP, Scott CJS, Walton JD (2002) Cellulose synthase-like genes of rice. Plant Physiol **128:** 336–340

Higuchi T (1997) Biochemistry and Molecular Biology of Wood. Springer, New York, pp 131–233

Hu WJ, Lung J, Harding SA, Popko JL, Ralph J, Stokke DD, Tsai CJ, Chiang VL (1999) Repression of lignin biosynthesis promotes cellulose accumulation and growth in transgenic trees. Nat Biotechnol **17:** 808–812

Jacobs A, Lundqvist J, Stalbrand H, Tjerneld F, Dahlman O (2002) Characterization of water-soluble hemicelluloses from spruce and aspen employing SEC/MALDI mass spectroscopy. Carbohydr Res **337:** 711–717

Keegstra K, Raikhel N (2001) Plant glycosyltransferases. Curr Opin Plant Biol **4:** 219–224

Kimura S, Laosinchai W, Itoh T, Cui X, Linder CR, Brown RM Jr (1999) Immunogold labeling of rosette terminal cellulose-synthesizing complexes in the vascular plant *Vigna angularis*. Plant Cell **11:** 2075–2085

Leloir LF (1951) The enzymatic transformation of uridine diphosphate glucose into a galactose derivative. Arch Biochem **33:** 186–190

Li L, Cheng XF, Leshkevich J, Umezawa T, Harding SA, Chiang VL (2001) The last step of syringyl monolignol biosynthesis in angiosperms is regulated by a novel gene encoding sinapyl alcohol dehydrogenase. Plant Cell **13:** 1567–1585

Liang X, Joshi CP (2004) Molecular cloning of ten distinct hypervariable regions from the cellulose synthase gene superfamily in aspen trees. Tree Physiol **24:** 543–550

Liepman AH, Wilkerson CG, Keegstra K (2005) Expression of cellulose synthase-like (Csl) genes in insect cells reveals that CslA family members encode mannan synthases. Proc Natl Acad Sci USA **102:** 2221–2226

Lu S, Sun YH, Shi R, Clark C, Li L, Chiang VL (2005) Novel and mechanical stress responsive microRNAs in *Populus trichocarpa* that are absent from Arabidopsis. Plant Cell **17:** 2186–2203

Madson M, Dunand C, Li X, Verma R, Vanzin GF, Caplan J, Shoue DA, Carpita NC, Reiter WD (2003) The *MUR3* gene of Arabidopsis encodes a xyloglucan galactosyltransferase that is evolutionarily related to animal exostosins. Plant Cell **15:** 1662–1670

McAloon A, Taylor F, Yee W, Ibsen K, Wooley R (2000) Determining the Cost of Producing Ethanol from Corn Starch and Lignocellulosic Feedstocks. National Renewable Energy Laboratory (NREL) Technical Report: NREL/TP-580–28893. National Renewable Energy Laboratory, Golden, CO

Nairn CJ, Haselkorn T (2005) Three loblolly pine CesA genes expressed in developing xylem are orthologous to secondary cell wall CesA genes of angiosperms. New Phytol **166:** 907–915

Nilsson LJ, Larson ED, Gilbreath KR, Gupta A (1995) Energy Efficiency and the Pulp and Paper Industry. Report No. IE962. American Council for an Energy-Efficient Economy, Washington, DC

Osakabe K, Tsao CC, Li L, Popko JL, Umezawa T, Carraway DT, Smeltzer RH, Joshi CP, Chiang VL (1999) Coniferyl aldehyde 5-hydroxylation and methylation direct syringyl lignin biosynthesis in angiosperms. Proc Natl Acad Sci USA **96:** 8955–8960

Pear JR, Kawagoe Y, Schreckengost WE, Delmer DP, Stalker DM (1996) Higher plants contain homologs of the bacterial *celA* genes encoding the catalytic subunit of cellulose synthase. Proc Natl Acad Sci USA **93:** 12637–12642

Peng L, Kawagoe Y, Hogan P, Delmer DP (2002) Sitosterol-β-glucoside as primer for cellulose synthesis in plants. Science **295:** 147–150

Perila O (1961) Chemical composition of carbohydrates in wood cells. J Polym Sci **51:** 19–26

Perrin RM, DeRocher AE, Bar-Peled M, Zeng W, Norambuena L, Orellana A, Raikhel NV, Keegstra K (1999) Xyloglucan fucosyltransferase, an enzyme involved in plant cell wall biosynthesis. Science **284:** 1976–1979

Perrin RM, Wilkerson C, Keegstra K (2001) Golgi enzymes that synthesize plant cell wall polysaccharides: finding and evaluating candidates in the genomic era. Plant Mol Biol **47:** 115–130

Ragauskas AJ, Williams CK, Davison BH, Britovsek G, Cairney J, Eckert CA, Frederick WJ Jr, Hallett JP, Leak DJ, Liotta CL, et al (2006) The path forward for biofuels and biomaterials. Science **311:** 484–489

Ranik M, Myburg AA (2006) Six new cellulose synthase genes from Eucalyptus are associated with primary and secondary cell wall biosynthesis. Tree Physiol **26:** 545–556

Richmond TA, Somerville C (2000) The cellulose synthase superfamily. Plant Physiol **124:** 495–498

Rydholm SA (1965) Pulping Processes. Interscience, London, pp 439–714

Samuga A, Joshi CP (2002) A new cellulose synthase gene (*PtrCesA2*) from aspen xylem is orthologous to *Arabidopsis AtCesA7* (*irx3*) gene associated with secondary cell wall synthesis. Gene **296:** 37–44

Sarkanen KV, Hergert HL (1971) Classification and distribution. *In* KV Sarkanen, CH Ludwig, eds, Lignins: Occurrence, Formation, Structure and Reaction. Wiley-Interscience, New York, pp 43–94

Saxena IM, Brown RM Jr (1997) Identification of cellulose synthase(s) in higher plants: sequence analysis of processive beta-glycosyltransferases with the common motif 'D,D,D35Q(R,Q)XRW'. Cellulose **4:** 33–49

Saxena IM, Brown RM Jr, Dandekar T (2001) Structure-function characterization of cellulose synthase: relationship to other glycosyltransferases. Phytochemistry **57:** 1135–1148

Saxena IM, Brown RM Jr, Fevre M, Geremia RA, Henrissat B (1995) Multidomain architecture of β-glycosyltransferases: implications for mechanism of action. J Bacteriol **177:** 1419–1424

Schlesinger WH, Lichter J (2001) Limited carbon storage in soil and litter of experimental forest plots under increased atmospheric CO_2. Nature **411:** 466–469

Shi R, Chiang VL (2005) A facile means for quantifying microRNA expression by real-time PCR. Biotechniques **39:** 519–525

Somerville C, Bauer S, Brininstool G, Facette M, Hamann T, Milne J, Osborne E, Paredez A, Persson S, Raab T, et al (2004) Toward a systems approach to understanding plant cell walls. Science **306:** 2206–2211

Taylor NG, Howells RM, Huttly AK, Vickers K, Turner SR (2003) Interactions among three distinct CesA proteins essential for cellulose synthesis. Proc Natl Acad Sci USA **100:** 1450–1455

Taylor NG, Laurie S, Turner SR (2000) Multiple cellulose synthase catalytic subunits are required for cellulose synthesis in Arabidopsis. Plant Cell **12:** 2529–2539

Taylor NG, Scheible WR, Cutler S, Somerville CR, Turner SR (1999) The *irregular xylem3* locus of Arabidopsis encodes a cellulose synthase required for secondary cell wall synthesis. Plant Cell **11:** 769–779

Thompson JD, Higgins DG, Gibson TJ (1994) CLUSTAL W: improving the sensitivity of progressive multiple sequence alignment through sequence weighting, positions-specific gap penalties and weight matrix choice. Nucleic Acids Res **22:** 4673–4680

Timell TE (1964) Wood hemicelluloses. Adv Carbohydr Chem **19:** 247–302

Timell TE (1969) The chemical composition of wood. Sven Papperstidn **72:** 173–181

Timell TE (1986) Compression Wood in Gymnosperms. Springer-Verlag, New York, pp 1–81; 289–408

Vanzin GF, Madson M, Carpita NC, Raikhel NV, Keegstra K, Reiter WD (2002) The *mur2* mutant of Arabidopsis thaliana lacks fucosylated xyloglucan because of a lesion in fucosyltransferase AtFUT1. Proc Natl Acad Sci USA **99:** 3340–3345

Wooley R, Ruth M, Sheehan J, Ibsen K, Majdeski H, Galvez A (1999) Lignocellulosic Biomass to Ethanol Process Design and Economics Utilizing Co-Current Dilute Acid Prehydrolysis and Enzymatic Hydrolysis Current and Futuristic Scenarios. National Renewable Energy Laboratory (NREL) Technical Report: NREL/TP-580–26157. National Renewable Energy Laboratory, Golden, CO

Wright PJ, Wallis AFA (1995) Rapid determination of carbohydrates in hardwoods by high performance anion exchange chromatography. Holzforschung **50:** 518–524

Wu L, Joshi CP, Chiang VL (2000) A xylem-specific cellulose synthase gene from aspen is responsive to tension stress. Plant J **22:** 495–502

Zhong R, Pena MJ, Zhou GK, Nairn CJ, Wood-Jones A, Richardson EA, Morrison WH III, Darvill AG, York WS, Ye ZH (2005) Arabidopsis *fragile fiber8*, which encodes a putative glucuronyltransferase, is essential for normal secondary wall synthesis. Plant Cell **17:** 3390–3408